

Seismic Performance Evaluation of Intake Towers

by

Richard C. Dove¹ and Enrique E. Matheu²

ABSTRACT

In the event of an earthquake, it is vitally important that the catastrophic failure of a dam and subsequent sudden release of the reservoir be prevented. An important part of the prevention of such a failure is maintaining the ability to control the release of water after the earthquake. For most earthen dams, and some concrete dams, the release of water is controlled through a reinforced concrete intake tower. The functional survival of such towers has been the main concern of a multi-year research effort sponsored by the U.S. Army Corps of Engineers (USACE). Most intake towers in the current USACE inventory are lightly reinforced. The functional survival of such lightly reinforced structures is thus the main concern of this research effort. The ultimate objective of this research work is the development of analysis procedures for seismic evaluation of these structures. This paper presents some of the results of this effort.

KEYWORDS: Reinforced concrete, ductility, intake towers, seismic evaluation, displacement-based approach, shaking table tests.

1. INTRODUCTION

Earthquake engineering research efforts in the area of reinforced concrete intake towers are currently focused on understanding the nonlinear response of lightly reinforced intake towers. The ultimate objective is the evaluation and/or development of simplified analysis procedures for the seismic evaluation of these structures. The work presented in this paper is part of a larger research effort that began with a statistical

analysis of the USACE inventory of existing intake towers. This tower inventory analysis quantified the distribution and variation of the structural characteristics of the towers as relating to their earthquake location hazard (Dove, 1996). The information collected was used in planning the second phase of this research program, referred to as the Intake Tower Substructure (ITS) experimentation series (Figure 1), which was conducted during 1996 and 1997 (Dove, 1998) at the Geotechnical and Structures Laboratory (Vicksburg, Mississippi).



Figure 1. Typical 1/8-scale static experiment.

The results from this experimental effort, which included monotonic and cyclic loading tests of 1/8-scale models, showed that substantial ductility is available (Figure 2). The objectives of these experiments were not only to observe the response of reduced scale models of typical intake towers and quantify the ductility available, but also to use the information generated for the development of approximate and/or simplified evaluation procedures for existing intake towers.

¹ Geotechnical and Structures Laboratory, U.S. Army Engineer Research and Development Center, Vicksburg, MS 39180 (USA).

² Department of Civil and Environmental Engineering, Louisiana State University, Baton Rouge, LA 70803 (USA).

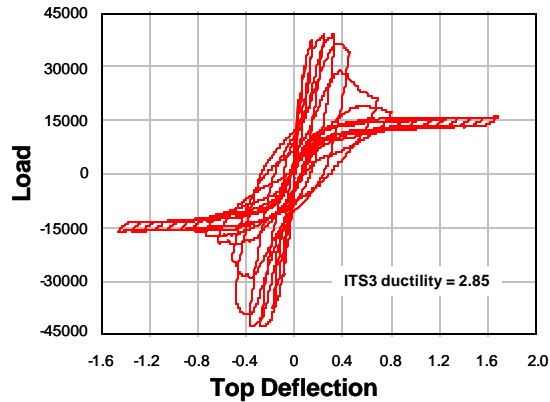


Figure 2. Typical load-deflection curve exhibiting substantial ductility.

Based on the results of the ITS experiments, it was concluded that additional information was required for the application of the simplified analysis procedures under development. Specifically, a method was needed to properly estimate the ultimate deflection capacity of existing intake towers. During 1999 and 2000, fourteen 1/2-scale experiments were conducted to provide a statistically significant basis for the development of an empirical estimation of the parameters needed (Dove, 2000). As a result of these tests, a modified displacement-based analysis procedure was generated incorporating the available experimental information. This analysis procedure is discussed in the next section. More recent research efforts have mainly focused on the validation and calibration of the proposed analysis procedure and its underlying assumptions by means of an extensive series of shaking table tests. The first series of tests were recently performed at the facilities of the Construction Engineering Research Laboratory (Urbana, Illinois). The corresponding results and preliminary conclusions are discussed in following sections.

2. DISPLACEMENT-BASED ANALYSIS

The nonlinear response and ductility of lightly reinforced intake towers has been the focus of recent analytical and experimental efforts. It has been shown that lightly reinforced intake towers can exhibit ductility but with a very localized failure. When a lightly reinforced intake tower is excited by a seismic event, a single crack forms

at the base of the tower or at the location of a major stiffness change. Experimentation has shown that ultimate failure is dependent on the response of the rebar within the crack (Dove, 2000). An analysis technique has been developed that reflects this localized failure mode and includes explicit consideration of the earthquake-induced displacements of a structure. It also attempts to account for the shift of the fundamental frequencies with formation of plastic regions in the structure. The proposed analysis procedure will be presented by applying it to a representative rectangular intake tower.

The structure analyzed has been used as an example problem in past and current USACE guidance documents (U.S. Army Corps of Engineers, 2002). The analysis presented here is essentially a modification of the prior analysis presented in this reference. The structure is a generic tapering rectangular tower about 61 m. tall, 14.6 m. by 11.6 m. wide with a wall thickness 1.83 m. at the base, as shown in Figure 3. Primary reinforcement consisted of #11 bars at 30.48 cm on center.

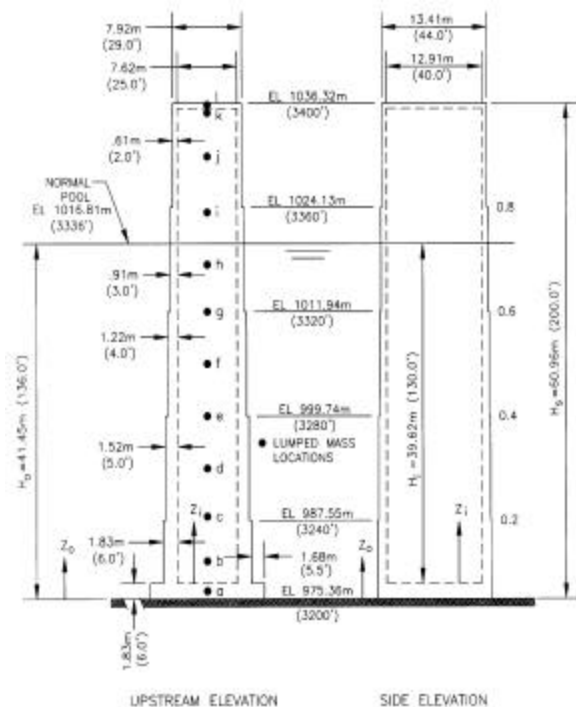


Figure 3. Layout of example intake tower.

The assumed analytical model consists of a simple cantilever beam attached to a rotational spring. The spring approximates the response of the cracked region. The beam models the response of the uncracked tower above the base. The definition of the rotational spring stiffness requires the calculation of the moment-curvature ($M-\phi$) relationship. Based on this relationship, it is then possible to calculate the corresponding moment-rotation relationship ($M-\theta$), which is obtained by multiplying the curvature by an assumed plastic hinge length. The $M-\theta$ relationship represents the stiffness of the rotational spring.

The $M-\theta$ relationship is often strongly bilinear, and therefore a simplification is required in order to conduct a response spectrum analysis. The $M-\theta$ relationship is linearized such that it encloses the same area for the same maximum rotation. This approximation allows the calculation of the expected deflection under the given earthquake loads. Given the linear spring stiffness, the element properties, and any added mass due to water, a response spectrum analysis can be readily conducted. The maximum deflection calculated represents the deflection demand of the tower under the input earthquake.

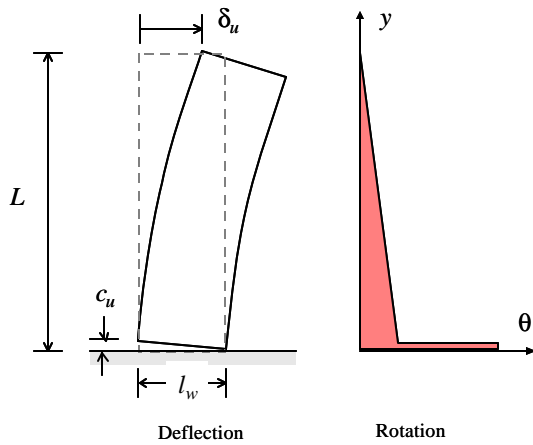


Figure 4. Deflection capacity.

In order to complete the analysis, it is necessary to determine the ultimate deflection capacity δ_u (Figure 4), which is calculated as follows:

$$\delta_u = \frac{\phi_E L^2}{3} + \delta_{cu} \quad (1)$$

where ϕ_E is the ultimate elastic curvature at the base of the tower, also known as the cracking curvature; θ_p represents the plastic rotation at failure; l_w denotes the depth of the section, L is the height of the intake tower; and δ_{cu} represents the deflection contribution caused by the base crack.

This model assumes that the ultimate lateral deflection consists of the sum of two parts. The first part is the elastic response of the body of the intake tower above the cracked section. The elastic curvature ϕ_E can be computed as

$$\phi_E = \frac{M}{EI_g} \quad (2)$$

where M denotes the yielding moment, E the elastic modulus, and I_g the uncracked moment of inertia. The second part is a rigid body rotation of the tower as the crack opens at the base of the elastic section, and the tower rotates about the neutral axis of the cracked section. It is conservative to assume that the neutral axis is coincident with the edge of the tower. Hence, the lateral rigid-body deflection at the top of the tower varies directly with the crack width, and its maximum value is as a ratio of the tower height and the tower width, times the ultimate crack width. Therefore,

$$\delta_{cu} = \theta_p L = \frac{c_u}{l_w} L \quad (3)$$

The principal unknown in the above equation is c_u , i. e., the ultimate crack width at failure, which is a function of the ultimate strain of the rebar and the strain penetration. Experiments have indicated that for a single crack response, the crack widths are largely predicted by the ultimate strain capacity of the rebar and rebar diameter. An empirical equation for c_u was generated as follows:

$$c_u = 0.12 + 2.47\varepsilon_u + 0.79d_b \quad (4)$$

where ε_u is the ultimate strain at failure of the rebar as measured over the standard gage length (20.3 cm or 8 inch) and d_b is the diameter of the reinforcing bar in cm.

Application of the proposed displacement-based procedure to the design example begins with the calculation of the $M-\phi$ relationship for the bottom section of the tower in two directions (weak and strong axis). This follows the assumption that the failure mechanism of the tower will be the formation of a single crack at the base of the bottom section. The vertical dead load of the tower self weight was included. Assuming an 18 percent ultimate strain, the ultimate crack width calculated from the above empirical equation to be 1.40 cm. The strain penetration length (L_s) can be calculated from the following equation:

$$L_s = \frac{c_u}{\epsilon_u} \quad (5)$$

This gives a strain penetration length of 7.52 cm. Multiplying the $M-\phi$ diagram by this strain penetration length gives the corresponding $M-\theta$ relationship. Proceeding as described above, the equivalent rotational spring stiffness is calculated such that the total area under the equivalent rotational spring is the same as that for the corresponding weak and strong axis $M-\theta$ relationships. The resulting equivalent spring constants are given by $2107E+12$ N-m/rad and $3.561E+12$ N-m/rad for the weak and strong axes, respectively. Based on these properties, and assuming a finite-element discretization of the structure using standard beam elements, a response spectrum analysis was conducted using the MDE response spectrum for 5% damping indicated in Figure 5. The results of this analysis indicate a top deflection of 9.6 cm for rotation about the strong axis and 10.1 cm for rotation about the weak axis.

Finally, it is necessary to calculate the ultimate deflection capacity δ_u . Given the ultimate crack width and section width at the base of the model, the ultimate base rotation θ_p can be calculated. The elastic curvature ϕ_E at the base of the intake tower (also known as the cracking curvature) is determined from the $M-\phi$ relationship for the section. Based on these parameters, the deflection capacity of the tower is calculated as 9.6 cm for rotation about the strong axis and 12.6 cm about the weak axis. Therefore, the tower passes the analysis.

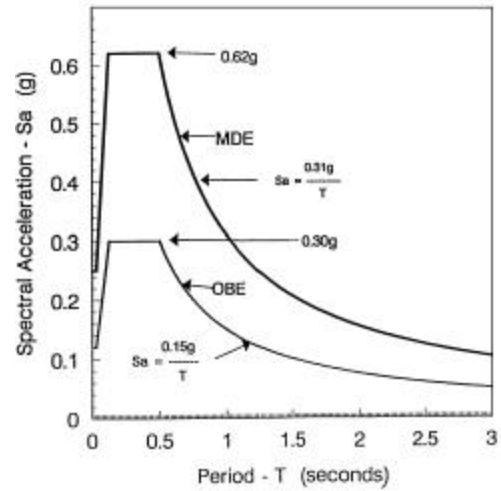


Figure 5. Standard spectra used in analysis.

3. SHAKING TABLE EXPERIMENTS

As part of a continuing effort to validate the displacement-based analytical procedure, a series of shaking table experiments were performed. The experiments were conducted on a 1/8-scale model of a typical intake tower, of the same design as used for the ITS3 cyclic loading tests. The objective of these tests was to compare the failure mode under dynamic conditions with the failure mechanism previously observed under monotonic and cyclic loading. These tests also served the purpose of providing additional data for the evaluation and validation of current analytical models.



Figure 6. Intake tower model on top of shaking table at the Construction Engineering Research Laboratory (Urbana, Illinois).

The tests were completed by early July 2001. The intake tower model (Figure 6) was tested laterally with uniaxial sinusoidal support motions, near the tower natural frequency in the short direction of the tower. Test levels were increased until failure occurred. Pre- and post-failure responses of the model as well as the corresponding failure mechanism were systematically documented. The extensive results collected from this testing program will facilitate a direct comparison between the measured responses and the behavior predicted by numerical models and previous static cyclic tests.

The intake tower model was 3.05 m tall with a hollow rectangular cross-section that was 1.32 m wide in the east-west direction and 1.02 m wide in the north-south direction. The walls were 0.14 m thick, constructed of normal strength concrete with scaled aggregate and reinforcing steel. The weight of the tower was calculated as 4.29 metric tons. Figure 7 shows a schematic drawing of the intake tower model, which was placed on top of a heavily reinforced base beam. The base beam was square, with a width of 2.74 m and a thickness of 0.46 m.

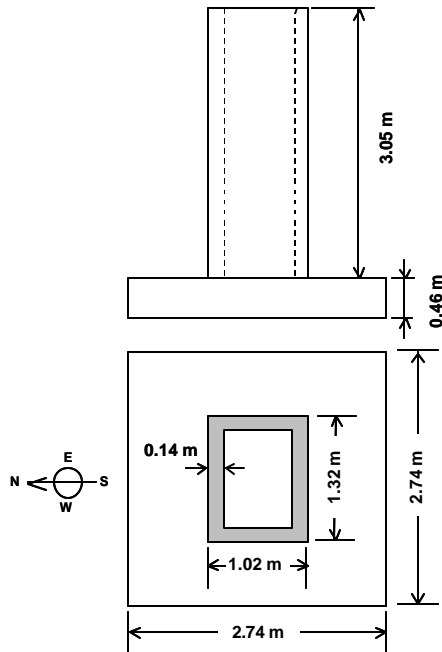


Figure 7. Schematic view indicating intake tower model dimensions.

The model was extensively instrumented with accelerometers attached to the base beam and the external faces, linear variable differential transducers (LVDT) installed between the base beam and tower, and several deflection gages. In addition, the vertical reinforcing steel was instrumented with strain gages. Progression of damage was extensively documented with digital photographs and video. Two digital camcorders were used: one recorded the overall model response from the east-north-east side, whereas the other camcorder zoomed in on the cold joint at the bottom of the model on the west face of the model (Figure 7).

Table 1. Scaling relationships

Variable	Scaling factors	
	$\lambda_L, \lambda_E, \lambda_\rho$	$\lambda_L, \lambda_E = \lambda_\rho = 1$
Time	$\lambda_t = \lambda_L \sqrt{\frac{\lambda_\rho}{\lambda_E}}$	$\lambda_t = \lambda_L$
Frequency	$\lambda_f = \frac{1}{\lambda_L} \sqrt{\frac{\lambda_E}{\lambda_\rho}}$	$\lambda_f = \frac{1}{\lambda_L}$
Force	$\lambda_F = \lambda_E \lambda_L^2$	$\lambda_F = \lambda_L^2$
Stress	$\lambda_\sigma = \lambda_E$	$\lambda_\sigma = 1$
Strain	$\lambda_\epsilon = 1$	$\lambda_\epsilon = 1$
Displacement	$\lambda_u = \lambda_L$	$\lambda_u = \lambda_L$
Velocity	$\lambda_{\dot{u}} = \sqrt{\frac{\lambda_E}{\lambda_\rho}}$	$\lambda_{\dot{u}} = 1$
Acceleration	$\lambda_{\ddot{u}} = \frac{\lambda_E}{\lambda_L \lambda_\rho}$	$\lambda_{\ddot{u}} = \frac{1}{\lambda_L}$

Table 1 displays the scaling relationships that govern this type of problem, in terms of 3 main scaling factors: λ_L (geometry), λ_E (modulus of elasticity), and λ_ρ (density). The model geometry was 1/8 of the prototype, that is, $\lambda_L = 8$. Standard strength concrete was used for the model, and therefore $\lambda_E = \lambda_\rho = 1$. The third column of the table contains the resulting scaling relationships for this case, which is characterized by an acceleration scaling factor that is the reciprocal of the geometric scaling factor. Therefore, inertial and gravity effects for the

model should be increased $\lambda_L = 8$ times with respect to prototype conditions. The scaling of inertial effects was achieved by increasing the magnitude of the imposed base accelerations by a factor of 8.

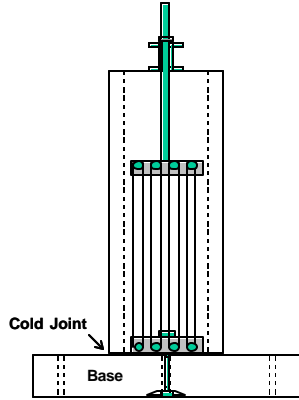


Figure 8. Schematic view depicting modeling of gravity load effects.

The scaling of gravity effects was achieved by means of 80 loops of 2.54cm diameter elastic cord connected between the top and the base of the tower model (Figure 8). The extremely flat load-deflection characteristics of these elastic cords allowed them to be used in such a way that the corresponding vertical loads did not vary significantly with the rocking response of the tower with respect to the base. The cords were designed to provide an additional vertical load equal to 30 metric tons. Including this load, the resulting vertical compressive stresses at the base of the model due to gravity effects were 575 kPa.

The model was initially tested with low-level random motions to measure natural frequencies, mode shapes and damping. These tests were conducted in the X (north-south) and Y (east-west) directions. The amplitude of these motions was initially selected very low (0.02 g), and the random motion tests were repeated at larger amplitudes until the modal information were clearly obtained in both horizontal directions.

The model was initially excited using sinusoidal base motions in the X direction at a frequency of 28 Hz (3.5 Hz, prototype scale). The imposed

base motions ramped up to full amplitude in 0.5 seconds; held a constant amplitude for 2.0 seconds; and ramped down in 0.5 seconds, for a total test duration of 3.0 seconds. For each test run, the amplitude of the sinusoidal support motion was gradually increased with respect to the previous one while keeping constant the excitation frequency. Previous static tests performed on similar 1/8-scale models indicated that the base of the model cracked at a value of top lateral deflection between 1.3 and 1.8 mm, with applied lateral loads between 130 and 170 kN.

The model failed by cracking at the cold joint at the base. Once it cracked across the entire cold joint surface, the model softened significantly. The change in the fundamental frequency was a very effective damage indicator. Damage evolution was carefully monitored by the LVDT measurements along the base of the model.

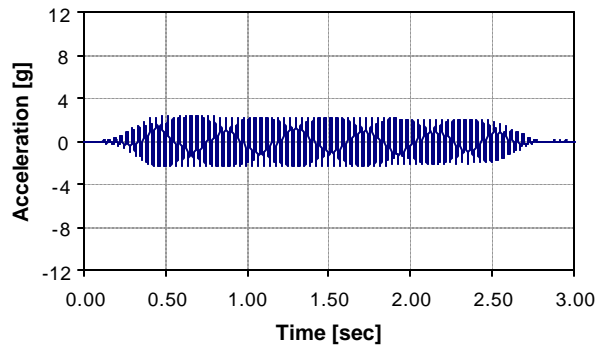


Figure 9. Base acceleration, A6x (run 18).

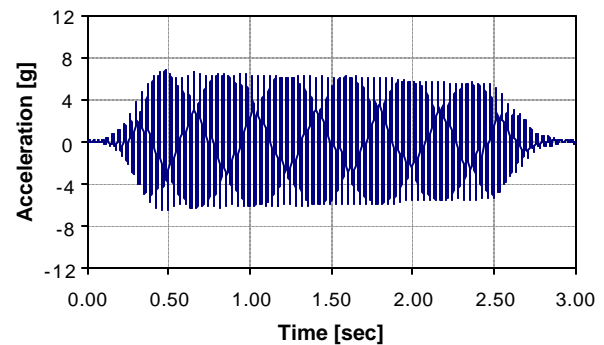


Figure 10. Top acceleration, A14x (run 18).

Figures 9 and 10 show acceleration responses measured during test run 18, corresponding to an excitation level of 2.04 g (0.255 g, prototype

scale). These responses correspond to sensors A6x and A14x, located at the bottom and top of the north face of the model, respectively. Figure 11 shows the time history measured by one of the deflection gages installed at the top of the model (D5x). The amplitude of oscillation is about 2 mm.

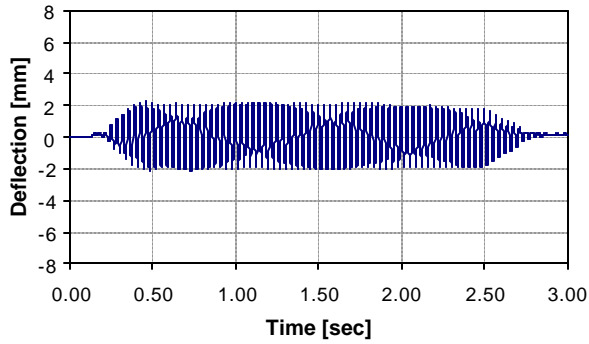


Figure 11. Top deflection, D5x (run 18).

After significant damage was identified, the model was again tested with random motions to determine updated modal properties associated with the damaged condition. Cracking of the model across the entire cold joint surface softened the structure, as evidenced by the shift in the fundamental vibration frequency. Figure 12 shows the transfer functions between the top model acceleration (A14x) and the base beam acceleration (A1x) corresponding to two different series of random motion tests. As shown in the figure, the fundamental frequency decreases from 29 Hz to 24 Hz.

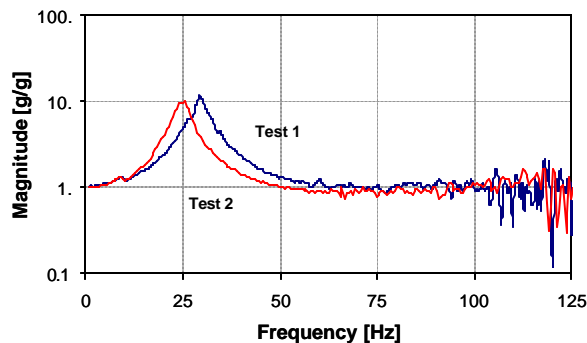


Figure 12. Transfer functions A14x/A1x for different series of random excitation tests.

Additional sinusoidal tests were conducted with an excitation frequency of 22 Hz (2.75 Hz,

prototype scale), gradually increasing the amplitude of the motions as in the previous case. Figures 13 and 14 show acceleration responses measured at the top and bottom of the model during test run 37, corresponding to an excitation level of 6.00 g (0.75 g, prototype scale).

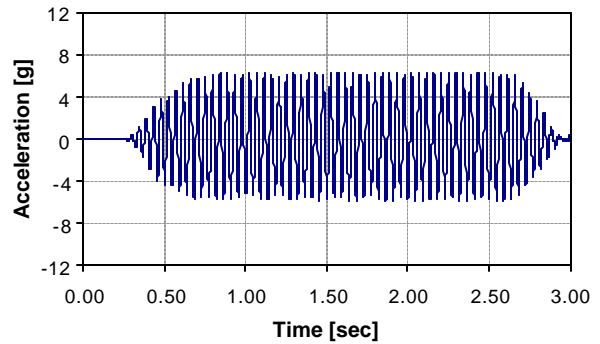


Figure 13. Base acceleration, A6x (run 37).

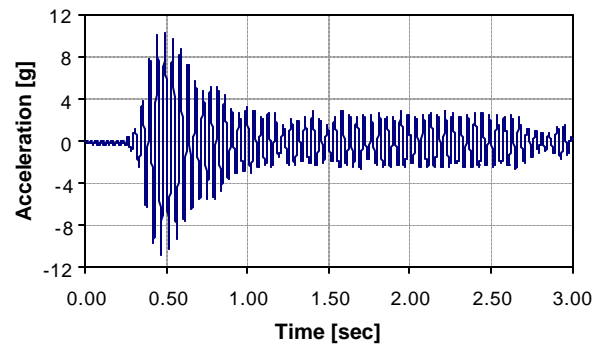


Figure 14. Top acceleration, A14x (run 37).

As seen in these figures, the behavior of the model at this stage exhibits different response characteristics that are induced by the significant damage and rotation at the base. Similar conclusions can be drawn by considering the top deflection of the model, shown in Figure 15.

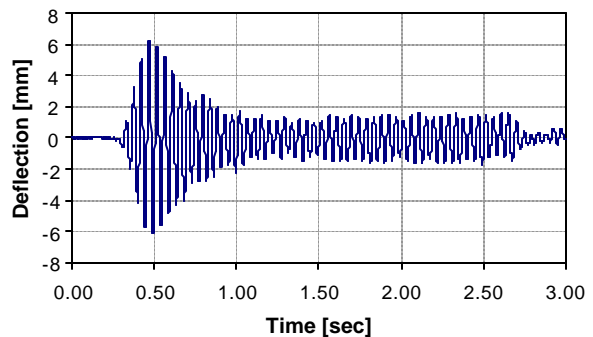


Figure 15. Top deflection, D5x (run 37).

Extensive quantitative information regarding the behavior of the failure surface (cold joint at the base of the model) was gathered by the vertical LVDT gages at that location. Figure 16 shows the time history for the sensor L2Z, illustrating the opening and closing of the single base crack.

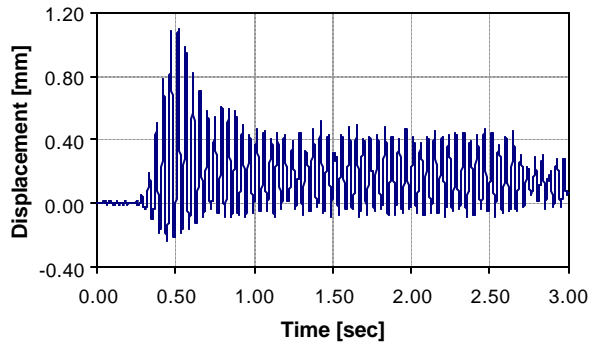


Figure 16. Base LVDT, L2z (run 37).

4. CONCLUSIONS

These experiments demonstrated that the failure mode under dynamic conditions was very similar to the failure mechanism previously observed under monotonic and cyclic loading. The same single crack response with significant ductility was witnessed in both the static and dynamic experiments. As expected the natural frequency of the model decreased substantially after cracking. The experiment validates the calculation of the deflection capacity based on the results of static experimentation. Future dynamic experiments will model the response of a tower to an individual earthquake. This will further validate the complete displacement-based analysis process.

5. ACKNOWLEDGEMENTS

This work was sponsored by the Direct–Allotted Civil Works Earthquake Engineering Research Program of the U.S. Army Engineer Research and Development Center (ERDC) in Vicksburg, Mississippi. The authors appreciate the cooperation of the authorities at the ERDC, which permitted the presentation and publication of this study. Permission to publish this paper was granted by the Chief of Engineers, U.S. Army Corps of Engineers.

6. REFERENCES

Dove, Richard C. (1996). “Structural Parameter Analysis of U.S. Army Corps of Engineers Existing Intake Tower Inventory,” Technical Report SL-96-1, U.S. Army Engineer Waterways Experiment Station, Vicksburg, MS.

Dove, Richard C. (1998). “Performance of Lightly Reinforced Concrete Intake Towers under Selected Loadings,” Technical Report SL-98-1, U.S. Army Engineer Waterways Experiment Station, Vicksburg, MS.

Dove, Richard C. (2000). “Performance of Lightly Reinforced Concrete Intake Towers under Selected Loadings,” Technical Report ERDC/SL TR-00-6, U.S. Army Engineer Research and Development Center, Vicksburg, MS.

Headquarters, U.S. Army Corps of Engineers (2002). “Structural Design of Spillways and Outlet Works,” Engineer Manual EM 1110-2-2400, Washington, DC (in publication).